

# Defective beams in MEMS: a model of non-ideal rods using a Cosserat approach for component level modelling

**Tim Gould and Charles H-T Wang**

Department of Physics, Lancaster University, Lancaster LA1 4YB

E-mail: [t.gould@lancaster.ac.uk](mailto:t.gould@lancaster.ac.uk), [c.wang@lancaster.ac.uk](mailto:c.wang@lancaster.ac.uk)

**Abstract.** We present and derive a technique for the introduction of defects into a beam model based on the Cosserat theory of rods. The technique is designed for the derivation of component models of non-ideal rods for use in MEMS devices. We also present a worked through example of blob/nick defects (where the rod has an area with an excess/lack of material) and a guide for a model with random pits and blobs along the length of the beam. Finally we present a component level model of a beam with a defect and compare it to results from a Finite Element Analysis simulation. We test the Cosserat model for two cases without any defect and four with a defect. Results are in good agreement with a maximum 0.5% difference for the ideal case and under 1% differences for all but one of the defective cases, the exception being a 2% error in an extreme case for which the model is expected to break down. Overall, the Cosserat model with and without defects provides an accurate way of modelling long slender beams. In addition, simulation times are greatly reduced through this approach and further development for both component level models as well as as FEA components is important for practical yet accurate modelling of MEMS both for prediction and comparison.

## 1. Introduction

Many MEMS devices rely on flexible rods of Si (or other materials) to act as a ‘spring’ for the device. As such, accurate models of such rods have been developed [1, 2, 3, 4] to facilitate simulation of these devices. Although these techniques can be quite sophisticated, so far work has concentrated on perfect (prismatic) rods i.e. those whose cross-sections do not change along the length and which have uniform material properties. While this is quite adequate for most common MEMS, such as the Tang Resonator where the system is designed to eliminate any *minor* defects caused by the manufacturing process, some more advanced devices may be quite susceptible to defects as may present designs if miniaturisation is to take place.

Presently, most simulation of such devices would be carried out using Finite Element Analysis through a package such as ANSYS®<sup>‡</sup> or FELT [5]. These simulations can be extremely time consuming both at the design level and during the calculation. Once defects are added it could be expected that the time required for design and to a lesser extent computation will increase dramatically.

Another approach to modelling is component level (or network) modelling [6, 7]. Here each component of a MEMS such as beams, shuttles, comb drives etc. are modelled individually and joined together. The resulting system requires finding the solution of a system of differential-algebraic equations (DAEs) [8] which is a relatively simple task. As such, component level modelling is very efficient for the modelling of new devices. Another aspect of component models is that they can also be introduced into FEA calculations to speed computation of certain ‘regions’ or ‘components’ of the system. Traditionally, beam models such as those of Euler-Bernoulli or Timoshenko [9] are used in these circumstances.

In this paper we propose a technique to model rods which builds on a recent model of beams based on Cosserat Theory [10] to introduce non-ideal properties such as defects caused by the manufacturing process. To demonstrate the viability of this method we provide two fully worked through and tested examples being a rod with a blob of excess material (or a ‘nick’ which is essentially the same problem) and a rod in which the manufacturing process has left a random jitter i.e. a series of minute pits and blobs with a known statistical distribution. We also run a series of tests on the blob/nick model where FEA simulations are used as a benchmark of the model developed in this paper.

The technique is designed to be easily implementable in a component level simulation, allowing it to be used in rapid modelling of present and future MEMS devices. The design of a ‘defective component’ can be carried out using this approach and installed into a preexisting model.

## 2. Preliminaries

In the modelling of flexible rods, the Cosserat approach is a good method for both analytic and numerical treatments. Through a kinematic assumption that the cross-sections of the rod change their orientation and position but not their shape along the length of the rod (physically reasonable in most cases) it is possible to write a Lagrangian for a rod as follows [10] (henceforth we use bold-italics for matrices and

<sup>‡</sup> ANSYS® is a registered trademark of ANSYS, Inc.

vectors with capitals for matrices and lowercase for vectors)

$$\begin{aligned}\mathcal{T} &= \int_0^L \frac{1}{2} A \partial_t \mathbf{r}^2 + \mathbf{w} \times A_\lambda \mathbf{d}_\lambda \cdot \partial_t \mathbf{r} + \frac{1}{2} \mathbf{w} \mathbf{I} \mathbf{w} \, ds \\ \mathcal{V} &= \int_0^L \frac{1}{2} (\mathbf{u} - \hat{\mathbf{u}}) \mathbf{K} (\mathbf{u} - \hat{\mathbf{u}}) + (\mathbf{u} - \hat{\mathbf{u}}) \mathbf{T} (\mathbf{v} - \hat{\mathbf{v}}) + \frac{1}{2} (\mathbf{v} - \hat{\mathbf{v}}) \mathbf{J} (\mathbf{v} - \hat{\mathbf{v}}) \, ds \\ \mathcal{L} &= \mathcal{T} - \mathcal{V}\end{aligned}\tag{1}$$

where  $\partial_s \mathbf{r} = \mathbf{u}$ ,  $\partial_s \mathbf{d}_i = \mathbf{u} \times \mathbf{d}_i$ ,  $\partial_t \mathbf{d}_i = \mathbf{w} \times \mathbf{d}_i$ ,  $\mathbf{K} = K_{ij} \mathbf{d}_i \otimes \mathbf{d}_j$ ,  $\mathbf{J} = J_{ij} \mathbf{d}_i \otimes \mathbf{d}_j$ ,  $\mathbf{T} = T_{ij} \mathbf{d}_i \otimes \mathbf{d}_j$  and  $\mathbf{I} = I_{ij} \mathbf{d}_i \otimes \mathbf{d}_j$ .  $t$  is time and  $s$  is a label for the position of a cross-section along the rod length (defined to run from 0 to  $L$  so that  $\Delta s = 1$  corresponds to one unit in the rest shape).  $\hat{\mathbf{u}}$  and  $\hat{\mathbf{v}}$  define the shape of the rod when no force is applied anywhere (reference configuration). We use Einstein summation convention where Greek letters are 1 or 2 and Roman letters range from 1 to 3 for the rest of this paper and repeated indices indicate sums eg.  $x_i y_i := \sum_{i=1}^3 x_i y_i$ .<sup>§</sup>

Finding the stationary point of the Lagrangian through the usual method with two variables yields the following coupled equations (three dimensions each leading to a six dimensional, second order linear PDE)

$$\begin{aligned}\partial_s \mathbf{n} + \mathbf{f} &= \rho A \partial_{tt} \mathbf{r} + \partial_{tt} \mathbf{q} \\ \partial_s \mathbf{m} + (\partial_s \mathbf{r}) \times \mathbf{n} + \mathbf{l} &= \mathbf{q} \times (\partial_{tt} \mathbf{r}) + \partial_t \mathbf{h}\end{aligned}\tag{2}$$

where  $\mathbf{f}$  and  $\mathbf{l}$  are external forces and torques and  $\mathbf{n}(s, t) = \partial_v \mathcal{V}(s, t)$ ,  $\mathbf{m}(s, t) = \partial_u \mathcal{V}(s, t)$ ,  $\mathbf{q} = A_\gamma \mathbf{d}_\gamma$  and  $\mathbf{h} = \mathbf{I} \mathbf{w}$ .

As in [3] we will adopt a quasi-static assumption. This means that we assume that all time-dependent terms in (2) (i.e. the RHS) are set to zero but the boundary conditions vary with time. In the context of MEMS modelling this assumption can be justified by realising that the frequencies of the entire, multi-component system, are significantly lower than the vibrational frequency of each component. This means that the wavelength of eigen modes is greater than half the length of the rods. With this assumption we reduce (2) to a six-dimensional, second order ODE which is much more amenable to analytic work than the complete PDE.

### 3. Material Perturbations

In order to introduce a defect we can introduce changes to any (or all) of: the shear and elastic moduli  $G$  and  $E$ ; the shape of the cross-section changing  $A$ ,  $A_\lambda$  and  $\mathbf{I}$ ; and the reference configuration through changes to  $\hat{\mathbf{u}}$  and  $\hat{\mathbf{v}}$ . Our technique involves introducing any of these changes as a perturbation to the ideal case. That is, we find a closest possible ideal case and treat differences as small. We can then expand (to increasingly higher orders if we like) the Cosserat equation in terms of the perturbation coefficient (which we denote  $\Gamma$ ) of the defect. The expansion in terms of  $\Gamma$  should then approach the complete solution as we increase the number of terms.

Noticing that any changes to the material will only affect  $\mathbf{n}$  and  $\mathbf{m}$ , we may rewrite (2) as (to first-order in  $\Gamma$ )  $\mathbf{n}(\mathbf{v}, \mathbf{u}) = \mathbf{n}^{(0)}(\mathbf{v}, \mathbf{u}) + \Gamma \mathbf{n}^{(1)}(\mathbf{v}, \mathbf{u})$  and  $\mathbf{m}(\mathbf{v}, \mathbf{u}) = \mathbf{m}^{(0)}(\mathbf{v}, \mathbf{u}) + \Gamma \mathbf{m}^{(1)}(\mathbf{v}, \mathbf{u})$  and then solve the Cosserat equations as a perturbation to the known system with  $\mathbf{n} = \mathbf{n}^{(0)}$  and  $\mathbf{m} = \mathbf{m}^{(0)}$ .

<sup>§</sup> The tensor quantities above take the following values:  $K_{\lambda\gamma} = \delta_{\lambda\gamma} G$ ,  $K_{\lambda 3} = K_{3\lambda} = 0$ ,  $K_{33} = E$ ,  $J_{\lambda\gamma} = \delta_{\lambda\gamma} E I_{\lambda\gamma}$ ,  $J_{\lambda 3} = J_{3\lambda} = 0$ ,  $J_{33} = G I_{33}$ ,  $T_{\lambda\gamma} = T_{33} = 0$ ,  $T_{13} = -E A_2$ ,  $T_{23} = E A_1$ ,  $T_{31} = G A_2$ ,  $T_{32} = -G A_1$  and  $I_{\lambda\gamma} = \delta_{\lambda\gamma} A_{\mu\mu} - A_{\lambda\gamma}$ ,  $I_{\lambda 3} = I_{3\lambda} = 0$ ,  $I_{33} = A_{\mu\mu}$ . Here  $A$  is the cross-sectional area,  $A_\lambda$  its first mass moments and  $A_{\lambda\gamma}$  are its second mass moments.

Keeping only the first-order terms and maintaining the quasi-static assumption we can now write

$$\begin{aligned}\partial_s \mathbf{n}^{(1)} &= 0 \\ \partial_s \mathbf{m}^{(1)} + \mathbf{A}(\mathbf{v}^{(0)})\mathbf{n}^{(1)} + \mathbf{A}(\mathbf{v}^{(1)})\mathbf{n}^{(0)} &= 0\end{aligned}\tag{3}$$

where

$$\begin{aligned}\mathbf{n}^{(1)} &= \mathbf{K}^{(0)}\Delta\mathbf{v}^{(1)} + \mathbf{K}^{(1)}\Delta\mathbf{v}^{(0)} + \left[\mathbf{A}(\mathbf{x}^{(1)}), \mathbf{K}^{(0)}\right]\Delta\mathbf{v}^{(0)} + \Delta\mathbf{u}^{(0)}\mathbf{T}^{(1)} \\ \mathbf{m}^{(1)} &= \mathbf{J}^{(0)}\Delta\mathbf{u}^{(1)} + \mathbf{J}^{(1)}\Delta\mathbf{u}^{(0)} + \left[\mathbf{A}(\mathbf{x}^{(1)}), \mathbf{J}^{(0)}\right]\Delta\mathbf{u}^{(0)} + \mathbf{T}^{(1)}\Delta\mathbf{v}^{(0)}\end{aligned}\tag{4}$$

and  $\Delta\mathbf{v}^{(I)} = \mathbf{v}^{(I)} - \hat{\mathbf{v}}^{(I)}$ ,  $\Delta\mathbf{u}^{(I)} = \mathbf{u}^{(I)} - \hat{\mathbf{u}}^{(I)}$  and  $\mathbf{A}(\mathbf{x}^{(1)}) = \mathbf{R}^{(0)}\mathbf{A}(\phi^{(1)})\mathbf{R}^{(0)T}$  ( $\mathbf{R}^{(0)} := \mathbf{R}(\phi^{(0)}) = \mathbf{d}_i^{(0)} \otimes \mathbf{e}_i$ ). Here the commutator term with  $\mathbf{A}(\mathbf{x}^{(1)})$  takes into account the effect of the change of basis set to first order.

This is then solved according to the boundary conditions  $\mathbf{r}^{(1)}(0) = \mathbf{r}^{(1)}(L) = 0$  and  $\phi^{(1)}(0) = \phi^{(1)}(L) = 0$ .

### 3.1. Series expansion in $\epsilon$

As in [3] let us make a first-order expansion in  $\epsilon$  (the perturbation coefficient of the boundary conditions) and substitute it into (4). We can now write

$$\begin{aligned}\Delta\mathbf{v}^{(0)} &= \epsilon\Delta\mathbf{v}^{(0,1)}, \Delta\mathbf{u}^{(0)} = \epsilon\Delta\mathbf{u}^{(0,1)} \\ \Delta\mathbf{v}^{(1)} &= \Delta\mathbf{v}^{(1,0)} + \epsilon\Delta\mathbf{v}^{(1,1)}, \Delta\mathbf{u}^{(1)} = \Delta\mathbf{u}^{(1,0)} + \epsilon\Delta\mathbf{u}^{(1,1)}\end{aligned}$$

Here the first upper index refers to powers of  $\Gamma$  and the second to powers of  $\epsilon$  and  $\mathbf{v}^{(0,0)} = \hat{\mathbf{v}}$ . We can justify the exclusion of terms above  $O(\epsilon)$  through the following argument: the expression we use for the ideal case is accurate to  $O(\epsilon^3)$ ; our expression is accurate to  $O(\Gamma\epsilon)$ ; assuming manufacturing to be quite precise then  $\Gamma \simeq O(\epsilon^2)$ ; thus the total accuracy for the non-ideal case  $\simeq O(\epsilon^3)$

Under these assumptions, equations (3) and (4) become  $\partial_s \mathbf{n}^{(1,0)} = 0$ ,  $\partial_s \mathbf{n}^{(1,1)} = 0$  and

$$\begin{aligned}\partial_s \mathbf{m}^{(1,0)} + \mathbf{A}(\mathbf{v}^{(0,0)})\mathbf{n}^{(1,0)} + \mathbf{A}(\mathbf{v}^{(1,0)})\mathbf{n}^{(0,0)} &= 0 \\ \partial_s \mathbf{m}^{(1,1)} + \mathbf{A}(\mathbf{v}^{(0,1)})\mathbf{n}^{(1,0)} + \mathbf{A}(\mathbf{v}^{(0,0)})\mathbf{n}^{(1,1)} \\ + \mathbf{A}(\mathbf{v}^{(1,1)})\mathbf{n}^{(0,0)} + \mathbf{A}(\mathbf{v}^{(1,0)})\mathbf{n}^{(0,1)} &= 0\end{aligned}$$

where

$$\begin{aligned}\mathbf{n}^{(1,1)} &= \mathbf{K}^{(0,0)}\Delta\mathbf{v}^{(1,1)} + \mathbf{K}^{(1,0)}\Delta\mathbf{v}^{(0,1)} + \Delta\mathbf{u}^{(0,1)}\mathbf{T}^{(1,0)} \\ &+ \left[\mathbf{A}(\mathbf{x}^{(1,0)}), \mathbf{K}^{(0,0)}\right]\Delta\mathbf{v}^{(0,1)} + \left[\mathbf{A}(\mathbf{x}^{(1,1)}), \mathbf{K}^{(0,0)}\right]\Delta\mathbf{v}^{(0,0)}\end{aligned}\tag{5}$$

$$\begin{aligned}\mathbf{m}^{(1,1)} &= \mathbf{J}^{(0,0)}\Delta\mathbf{u}^{(1,1)} + \mathbf{J}^{(1,0)}\Delta\mathbf{u}^{(0,1)} + \mathbf{T}^{(1,0)}\Delta\mathbf{v}^{(0,1)} \\ &+ \left[\mathbf{A}(\mathbf{x}^{(1,0)}), \mathbf{J}^{(0,0)}\right]\Delta\mathbf{u}^{(0,1)} + \left[\mathbf{A}(\mathbf{x}^{(1,1)}), \mathbf{J}^{(0,0)}\right]\Delta\mathbf{u}^{(0,0)}.\end{aligned}\tag{6}$$

## 4. Examples

### 4.1. ‘Blobs’ and ‘Nicks’

Sometimes a rod might be created with a bump of extra material or a nick through errors in the manufacturing process. This would locally affect the mass moments of

the rod so that we would have to use  $A(s)$ ,  $A_\gamma(s)$  and  $A_{\gamma\lambda}(s)$  to calculate  $\mathbf{K}$ ,  $\mathbf{J}$  and  $\mathbf{T}$ .

Treating this defect as a small perturbation from an otherwise uniform cross-section we can write

$$\mathbf{K} = \mathbf{K}^{(0,0)} + \Gamma \mathbf{K}^{(1,0)}(s), \quad \mathbf{J} = \mathbf{J}^{(0,0)} + \Gamma \mathbf{J}^{(1,0)}(s), \quad \mathbf{T} = \Gamma \mathbf{T}^{(1,0)}(s)$$

where  $\mathbf{K}^{(0,0)} = K_{ij}^{(0,n0)} \mathbf{d}_i^{(0,0)} \otimes \mathbf{d}_j^{(0,0)}$  and  $\mathbf{K}^{(1,0)} = K_{ij}^{(1,0)}(s) \mathbf{d}_i^{(0,0)} \otimes \mathbf{d}_j^{(0,0)}$  while  $K_{ij}^{(1,0)}(s) = K_{ij}^{(1,0)} \text{dist}(s)$  (same for  $\mathbf{J}$  and  $\mathbf{T}$ ). Note that  $\mathbf{T}^{(0,0)} = 0$  as we choose the path of the ideal rod to follow the centre-of-mass of the fixed cross-sections.

Let us find a solution to (3) where the rod deviates slightly from its reference frame (to order  $\epsilon$ ) due to displacements and rotations of its end points. We substitute

$$\begin{aligned} \Delta \mathbf{v}^{(0,0)} &= \epsilon \mathbf{v}^{(0,1)}, \Delta \mathbf{u}^{(0,0)} = \epsilon \mathbf{u}^{(0,1)} \\ \Delta \mathbf{v}^{(1,0)} &= \epsilon \mathbf{v}^{(1,1)}, \Delta \mathbf{u}^{(1,0)} = \epsilon \mathbf{u}^{(1,1)} \end{aligned}$$

into (5) and (6) (here the terms involving commutators vanishes as  $\mathbf{A}(\mathbf{x}^{(1,0)})$  is by definition  $O(\epsilon)$  and must therefore be multiplied by  $\Delta \mathbf{v}^{(0,0)} = 0$ ) as follows

$$\begin{aligned} \mathbf{n}^{(1,1)} &= \mathbf{K}^{(0,0)}(\mathbf{v}^{(1,1)} - \hat{\mathbf{v}}^{(1,1)}) + \mathbf{K}^{(1,0)}(\mathbf{v}^{(0,1)} - \hat{\mathbf{v}}^{(0,1)}) + \mathbf{T}^{(1,0)\text{T}} \mathbf{u}^{(0,1)} \\ \mathbf{m}^{(1,1)} &= \mathbf{J}^{(0,0)} \mathbf{u}^{(1,1)} + \mathbf{J}^{(1,0)} \mathbf{u}^{(0,1)} + \mathbf{T}^{(1,0)}(\mathbf{v}^{(0,1)} - \hat{\mathbf{v}}^{(0,1)}) \end{aligned}$$

which may then be used to calculate  $\mathbf{v}^{(1,1)}$  and  $\mathbf{u}^{(1,1)}$ .

After some work we can obtain expressions for  $\phi^{(1,1)}$  and  $\mathbf{r}^{(1,1)}$  were we have made an assumption that the shape of the perturbations distribution is governed by the same function of  $s$  for each of  $\mathbf{K}$ ,  $\mathbf{J}$  and  $\mathbf{T}$  (this is completely true for nicks and blobs). The solutions are thus given by

$$\begin{aligned} \mathbf{J}^{(0,0)} \phi^{(1,1)} &= \mathbf{k}_m^{(1,0)} s - \mathbf{A}_3 \mathbf{k}_n^{(1,0)} \frac{s^2}{2} \\ &\quad - \mathbf{J}' \left( \mathbf{k}_m^{(0,0)} \tilde{\mathbf{I}} - \mathbf{A}_3 \mathbf{k}_n^{(0,0)} \tilde{s} \right) - \mathbf{T}' [\mathbf{K}^{(0,0)}]^{-1} \mathbf{k}_n^{(0,0)} \tilde{\mathbf{I}} \\ \mathbf{K}^{(0,0)} \mathbf{r}^{(1,1)} &= \mathbf{K}^{(0,0)} \mathbf{A}_3 \int_0^s \phi^{(1,1)} ds' + \mathbf{k}_n^{(1,0)} s - \mathbf{K}' \mathbf{k}_n^{(0,0)} \tilde{\mathbf{I}} \\ &\quad - \mathbf{T}'^{\text{T}} [\mathbf{J}^{(0,0)}]^{-1} (\mathbf{k}_m^{(0,0)} \tilde{\mathbf{I}} - \mathbf{A}_3 \mathbf{k}_n^{(0,0)} \tilde{s}) \end{aligned} \tag{7}$$

where  $\tilde{f}(s) = \int_0^s f(s') \text{dist}(s') ds'$ . We can calculate  $\mathbf{k}_n^{(1,0)}$  and  $\mathbf{k}_m^{(1,0)}$  ( $\mathbf{k}_n^{(0,0)}$  and  $\mathbf{k}_m^{(0,0)}$  are known from the ideal case) by ensuring that  $\phi^{(1,1)}(L) = 0$  and  $\mathbf{r}^{(1,1)}(L) = 0$ . The full analytic solutions are far too complicated for inclusion here although the MAPLE source to generate them is available on request.

Figure 1 shows a visual demonstration of the model were we have calculated the bending properties of a beam of certain dimensions and boundary conditions both with and without a defect. The difference is, as expected, greatest around the position of the defect itself. Both the change in shape, and potential energy from the defect itself will affect the restoring force of the beam.

#### 4.2. Random jitter

The treatment of random jitter is all but identical to that of a localised defect such as a blob or nick. The only difference is that the distribution function  $\text{dist}(s)$  will have different expectation values which depend on the type and magnitude of the noise (eg. we may have  $\bar{\mathbf{I}} = \int_0^L \text{dist}(s) ds = 0$  whereas  $\bar{s} = k$ ). Substituting these values into the

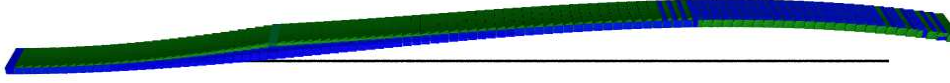


**Figure 1.** Model of a beam demonstrating its shape when it contains/does not contain a defect. The blue represents the ideal case while the green beam has a defect located at the marked point.

final expressions (which we have not included here) we can calculate the behaviour of the rod. Although beyond the scope of this paper, the same model will also be applicable to the calculation of noise ‘distributions’.

This second example demonstrates the power of the technique as the same equations can be used for two different types of physical impurities. Other impurities can be modelled in similar ways by changing the ‘noisy’ variable.

## 5. Implementation

One of the main advantages of the method outlined in [4] is that it gives us a means to convert the internal structure of a rod into a generalised force dependent only on the value of the end points (position and orientation of each end). This allows us to easily generate a component model of the rod for use in a component level simulator.

Using MAPLE we can follow the same procedure to derive analytic expressions for the change to the effective spring matrix of the end points (a  $12 \times 12$  matrix) caused by a defect. We then add our new term to the third-order expression from [4] and create a VHDL-AMS file representing the defective rod. This is then compiled through a component level simulator (SMASH 5.2.0<sup>TM</sup>||) and can be connected to other components.

The expression for the change in potential energy from the defect can be written as

$$\begin{aligned} \mathcal{V}^{(1,0)} = \int_0^L [ & \mathbf{n}^{(1,0)} \cdot \Delta \mathbf{v}^{(0,0)} \mathbf{m}^{(1,0)} \cdot \Delta \mathbf{u}^{(0,0)} - \frac{1}{2} \Delta \mathbf{v}^{(0,0)} \mathbf{K}^{(1,0)} \Delta \mathbf{v}^{(0,0)} \\ & - \frac{1}{2} \Delta \mathbf{u}^{(0,0)} \mathbf{J}^{(1,0)} \Delta \mathbf{u}^{(0,0)} - \frac{1}{2} \Delta \mathbf{u}^{(0,0)} \mathbf{T}^{(1,0)} \Delta \mathbf{v}^{(0,0)} ] ds \end{aligned} \quad (8)$$

and we ignore the change to kinetic energy so that  $\mathbf{F}^{(1,0)} = \mathbf{K}^{(1,0)} \mathbf{Q}$  where  $\mathbf{K}^{(1,0)} = \partial_{\mathbf{Q}} \partial_{\mathbf{Q}} \mathcal{V}^{(1,0)}$ . Here  $\mathbf{Q} := [x_1, y_1, z_1, \phi_{x1}, \phi_{y1}, \phi_{z1}, x_2, y_2, z_2, \phi_{x2}, \phi_{y2}, \phi_{z2}]$  where  $x_1$  etc. are the changes to the boundary conditions at the two ends of the beam.

## 6. Results

In order to verify the applicability and accuracy of the defect model (and for that matter the ideal Cosserat model) we compare the results of FEA simulations with those of the component model. We compare six different slender beams, each a variation of a length  $150\mu\text{m}$ , width  $6\mu\text{m}$  and height  $15\mu\text{m}$  beam (see Figure 2). These dimensions are quite typical of MEMS devices although we use a shorter beam to ensure that the FEA calculations run quickly (about one hour on a 2.80GHz Pentium 4 with

|| SMASH is trademarked to Dolphin Integration

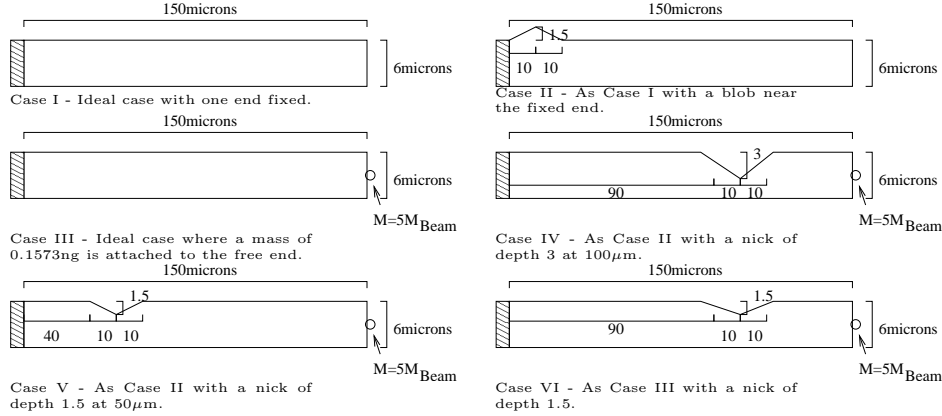


**Figure 2.** Diagrams of the Test Cases. Each of these is a variant of Case I and the height (15 $\mu\text{m}$ , not pictured) remains unchanged throughout. In all cases we consider the lowest energy mode where the motion is in the plane of the diagrams.

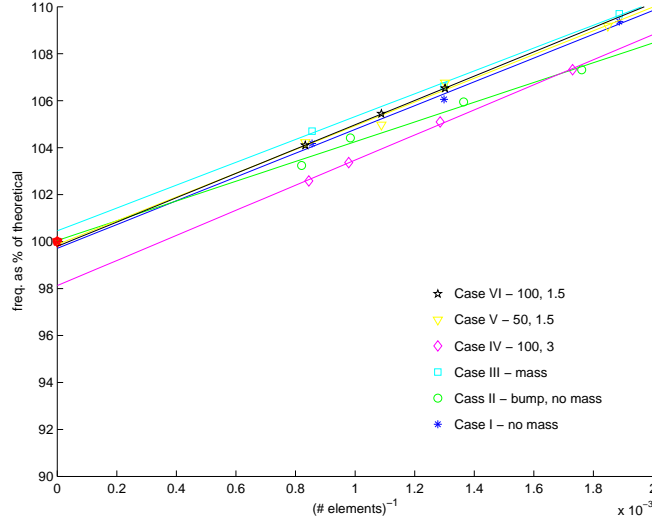


**Figure 3.** Graphs of FEA calculations and their extrapolated values where the frequencies are renormalised to a percentage of the Cosserat value.

1GB RAM for the longest calculations) with a decent accuracy. All simulations are performed in FELT [5] and it is worth noting that the solution of the Cosserat model takes an imperceptible amount of time on the same computer.

As a first test we must determine the accuracy of the Cosserat model of an ideal beam. For this purpose we must consider the result of a ‘perfect’ (i.e. one with an infinite number of elements in the beam) FEA calculation. For this purpose we must extrapolate the results of FEA calculations to infinity. We assume that for any FEA calculation, the result will take the form  $f_{\text{FEA}} = f_{\infty} + \delta/(\text{number of triangular elements})$ . With this assumption it is possible to calculate  $f_{\infty}$  by extrapolating a number of calculations with varying numbers of elements. This

involves making a linear fit to  $f_{\text{FEA}}$  versus  $1/\#\text{elements}$ . Figure 3 demonstrates the validity of this method. It is quite apparent from the graphs that the FEA results lie close to a straight line for all six cases. Of further assurance is the fact that  $\delta$  is positive in all cases. This is as expected since an FEA calculation will necessarily be more restrictive than the infinite case and must produce a higher lowest-mode frequency.

We summarise the results of our calculations in Table 1. Considering first the two ideal cases (I and III, without and with an attached mass respectively) we see that the Cosserat model is a highly accurate model of a beam. In both cases it agrees to within 0.5% of the extrapolated FEA result ( $f_{\infty}$ ). This is well within the error bounds of the extrapolation technique.

System	$f_{\infty}$ (GHz)	$f_{\text{Coss}}$ (GHz)	% Err
I	334.2	335.3	0.29
II	358.3	358.1	-0.045
III	72.18	71.85	-0.46
IV	69.16	70.48	1.9
V	69.28	69.37	0.13
VI	71.08	71.22	0.21

**Table 1.** Results of the FEA and Cosserat Simulations.

Moving on to the defect model we observe that the results of the Cosserat model or similarly close to those of the FEA simulations for all cases but IV. The ‘poor’ accuracy of Case IV is easily understood by considering that we have chosen an extreme case which goes beyond the expected range of the perturbation technique used. A defect this large (half the width of the beam) would not occur in a real MEMS device and would almost certainly cause significant problems (such as a full breakage) beyond the applicability of any beam model.

## 7. Conclusion

In this paper we have developed a technique for the construction of beam models with defects. We apply this technique to the construction of a model of a beam with a blob/nick present as well as a model of a beam with random jitter.

The theoretical framework presented can be effectively applied to new cases for the development of new models. This allows us to devise models for defects which are presently unobserved (such as kinks in a beam), but which may cause problems in future devices, particularly those made of novel materials or with novel applications.

The developed blob/nick and random jitter models could be used for reliability tests of MEMS both at the design and production stage. This is particularly valuable in the modelling of high specification MEMS, where an accurate model of faults is vital for the design process as costs are high for experiments.

Tests on the blob/nick model show that the model is a highly accurate tool for the simulation of such systems. An accuracy of at worst 0.5% for all but the most extreme case (which would not appear in practice) suggests that the model is more than satisfactory for simulation of real devices through Component Level Simulations or FEA simulations.



One possible future use of this technique would be to develop a model of a curved beam with a defect. At present, curved beams present difficulties for standard techniques of ideal beams. The Cosserat model has already been applied to curved beam models [11] and application of the aforementioned technique to this work may allow accurate modelling of future MEMS devices such as accelerometers.

### Acknowledgements

We would like to thank Richard Rosing at Lancaster University and colleagues at QinetiQ (Malvern) and ST Microelectronic (Milan) for helpful discussions. The work is funded by the EPSRC under the Computational Engineering Mathematics Programme.

- [1] CoventorWare of Coventor Inc. <http://www.coventor.com>.
- [2] MEMSMaster of MEMSCAP, <http://www.memscap.com>.
- [3] Wang C, Liu D, Rosing R, Richardson A and DeMasi B 2004 Construction of nonlinear dynamic MEMS component models using Cosserat theory Analog Integrated Circuits and Signal Processing, In press
- [4] Cao D Q, Liu D and Wang C H-T Computational Cosserat Dynamics in MEMS Component Modelling Proc 6th World Congress of Computational Mechanics, Beijing, 2004
- [5] FELT - open source FEA code, <http://felt.sourceforge.net/>.
- [6] Lorenz G and Neul R 1998 Network-Type Modeling of Micromachined Sensor Systems, Proc. of the MSM, pp. 233–238, April 1998, Santa Clara.
- [7] Mukherjee T, Fedder G K and Blanton R D 1999 Hierarchical Design and Test of Integrated Microsystems, IEEE Design and Test of Computers, **16** 18
- [8] Brenan K E, Cambell S L and Petzold L R 1996 Classics in Applied Mathematics 14, SIAM. Numerical solution of initial-value problems in differential-algebraic equations.
- [9] Timoshenko S. P. and Gere J. E. 1961 Theory of Elastic Stability. (New York: McGraw-Hill).
- [10] Antman S. 1991 Non-linear Problems in Elasticity, Applied Mathematical Sciences 107. (N.Y.: Springer-Verlag).
- [11] Tucker R W and Wang C H-T 2003 Gravitational wave induced vibrations of slender structures in space Gen. Rel. Grav. **35** 2137